ELSEVIER

Thermochimica Acta 367–368 (2001) 297–309

thermochimica acta

www.elsevier.com/locate/tca

Thermal analysis of ground dolomite, confirmation of results using an X-ray powder diffraction methodology

M. Samtani, E. Skrzypczak-Janktun, D. Dollimore[†], K. Alexander[*]

Department of Chemistry, College of Pharmacy, The University of Toledo, 2801 W Bancroft St., Toledo, OH 43606 3390, USA

Received 19 October 1999; accepted 20 July 2000

Abstract

Grinding is one of the most widely used unit processes in industry. The application of grinding to the pharmaceutical industry is investigated in detail. The process of grinding finds wide application because it leads to surface activation and particle size reduction. This objective is achieved by the application of energy. A lot of the applied energy is dissipated as heat. A number of pharmaceutical solids are known to be heat labile. Thus, the milling operation is a high-energy process, which could lead to detrimental effects on the structural pattern of the material being ground. This could be either due to the heat involved in the milling process or simply because of the high-energy impact of the milling medium. To investigate if grinding had detrimental effects, a detailed study was carried out using dolomite as the material to be ground. The unit cell of dolomite remained intact even after 24 h of grinding in a high-energy vibrating mill. This fact was confirmed using an X-ray powder diffraction methodology. It was found that although grinding did not deform the structural pattern of the dolomitic unit cell, a strain was however introduced in the structure. This strain appeared as a third peak in both the DTG and OTA curves This indicated the possible hazards of prolonged grinding and use of high-energy grinding equipment on the material exposed to the grinding process.

Keywords: Dolomite; Grinding; TG; DTA; X-ray powder diffraction; SEM

1. Introduction

Dolomite is a pharmaceutical excepient. It is used as a calcium and magnesium supplement in the pharmaceutical industry [1]. The $MgCO_3$ part of the dolomitic structure functions as a source of Mg to microorganisms and is therefore used as an additive for fertilizer [2]. For the same reason it is also used as an additive for food and is a common ingredient in health foods. Our objective is to investigate if grinding could prove detrimental to a substance having a high degree of hardness. If this could be proved, then it would strongly indicate that high-energy grinding can, in fact, be hazardous and can cause structural damage. Dolomite ("James White River Dolomite" supplied by FMC Corp/PD, Newark, DE 19711) being of rocky origin is a very hard material and was therefore the substance of choice for this study.

A literature survey of studies performed on ground dolomite indicates that grinding can lead to crystal structure alteration in dolomite. The magnesium carbonate portion of the dolomite structure degenerates into two distinct phases. These two phases are referred to as Mg I and Mg II [3]. Ozao et al. [4] in their work conclude that thermal analysis is sensitive to two different phases of magnesium carbonate decomposition

---

[*] Corresponding author.

E-mail address: kalexan@utnet.utoledo.edu (K. Alexander).

[†] Deceased

PII: S0040-6031(00)00663-8

but these are not positively distinguished by XRD and IR analysis. Arai and Yasue [5–7] have observed that the DTA peak due to magnesium carbonate splits into two. The new peak occurs at a lower temperature and as the period of grinding increases the new peak grows in intensity at the expense of the original peak. The final result is a single peak at the lower temperature. This stage is called 'the attainment of a new equilibrium', by the above authors.

It is found in three different instances in the literature [3,4,8] that the X-ray powder diffraction (XRD) peak intensities decrease with an increase in grinding time. Bradley et al. [8] proposed that this is due to cation displacements which leads to the formation of magnesium carbonate rich portions in the structure of dolomite. Kristóf and Jahász [3] examined the structural alterations in dolomite in a detailed study involving complex analytical methods. They showed from their XRD results that the reaction of the {0 0 6} lattice planes characterizing the successive Ca–Mg layers changes to the greatest extent. They concluded that because of the distortion of the {0 0 6} lattice planes the $\text{–O–Mg}^{+2}\text{–O–}$ bonds are weaker. Molchanov [9] found that a mechanochemical reaction occurs in dolomite wherein dolomite disintegrates into its component carbonates.

There is speculation regarding the nature of ground dolomite and what structural changes occur upon grinding. To detect possible changes upon grinding an XRD technique was used. Our aim is to determine if grinding had induced any structural damage in the dolomitic structure. To detect any structural change silicon metal was used as a reference standard. A 10% w/w silicon was introduced in all the dolomite samples and then the XRD was performed on these mixtures. The rationale for adopting this methodology is as follows.

The crystal lattice orientation in a powder sample causes the X-rays to scatter in a reproducible fashion at distinct angles relative to the incident X-rays [10]. If the grinding process affected the crystal structure of dolomite then the pattern of the scattered X-rays would be different as compared to the original dolomite sample. This difference could be either in the intensity of the peaks or the position of the peaks. The problem faced while doing XRD was that it is vulnerable to manual loading of the sample. If the sample is slightly leveled above or below the optical center of the instrument the peaks can shift either to the left or right. It is crucial therefore to distinguish experimental errors from the true variations in the structure. Thus, an internal standard had to be chosen to enable calibration of the diffraction patterns. The computer program 'Peak finder' in the suit of programs connected to the X-ray powder diffractometer is capable of applying corrections to the detected peaks based on an internal standard. As already noted, silicon metal was chosen as the internal standard. For example, if the peaks of dolomite were to shift due to variations in the sample depth in the sample holder then a similar shift would also occur for the silicon peaks. After application of the correction this effect would be negated and only genuine shifts in the peaks of dolomite would be detected.

2. Literature review

2.1. Principles of grinding, grinding in the pharmaceutical industry and its limitations

Grinding results in a change of state of the material being ground. The effect of grinding can be classified into two groups [4,11]:

1. A beneficial effect wherein there is very little crystal structure change and the grinding energy causes a reduction in particle size. This causes an increase in surface area and surface activation, which is a highly desirable process.
2. A detrimental effect which leads to the formation of cracks, changes in crystal structure, formation of strain within the structure, partial decomposition, increased crystal defects, phase transition, etc. All these lead to a change in the physicochemical properties of the material being ground.

The three laws governing grinding are Kick's law, Rittenger's law and Bond's law and are noted in that order, [12].

1. *Kick's Law* states that "The work required to reduce the size of a given quantity of material is constant for the same reduction ratio regardless of the original size of the initial material." Kick's law may be expressed as [10]

$$E = C\ln\left(\frac{D_1}{D_2}\right) \tag{1}$$

where E is the energy requirement; C the reciprocal efficiency coefficient, $C = K_k f_c$; K_k the Kicks constant; f_c the crushing strength of the material; D_1 and D_2 are the diameters of feed material and discharged product, respectively.

2. *Rittinger's Law* states that "The work used for particulate size reduction is directly proportional to the new surface produced." Rittenger's law is expressed by the following equation [10]:

$$E = k_1(S_2 - S_1) \tag{2}$$

where k_1 includes the relationship between particle surface and diameter; S_1 and S_2 are the specific surface before and after milling.

In terms of particle diameter the equation can be written as [10]

$$E = C'\left(\frac{1}{D_2} - \frac{1}{D_1}\right) \tag{3}$$

where $C' = K_r f_c$; K_r the Rittenger's constant.

3. *Bond's Law* states that "The work used to reduce the particle size is inversely proportional to the square root of the diameter of the particles produced." Bond's law may be expressed mathematically as follows [10]:

$$W_t \propto \frac{1}{\sqrt{D_2}} \tag{4}$$

where, W_t is the total work of comminution in kilowatt-hours per short ton of milled material; D_2 the size in microns through which 80% by weight of the milled product will pass.

The following is a brief account of the many applications of grinding to the pharmaceutical industry. Grinding increases the surface area, which influences the rate of reaction between the various components of a chemical reaction during a manufacturing process [13]. Orally administered drugs must first dissolve before they can be absorbed. The dissolution rate of orally administered formulations is governed by the particle size [13]. This is particularly true for drugs with low solubility. The classic example is that of griseofulvin. The control of fineness of griseofulvin led to an oral dosage regimen which was half that of the originally marketed product [14]. If the drug is to be extracted from a naturally occurring substance or from a natural source such as an animal gland then the rate of extraction depends upon the particle size. Reduced particle size greatly reduced the time of extraction [10].

Cosmetic products should also have an aesthetic appeal. In order to enhance the aesthetic appeal, impalpability and ease of spreading are two desirable characteristics [13]. Both of these are affected by an increase in particle size. Therefore, cosmetic powders should have reduced particle size and generally should be finer than 30 μm [13]. A number of properties of suspensions depend on the particle size of the dispersed phase. For suspensions a critical particle size should be maintained because a large particle size causes settling of the particles. Sedimentation is a function of particle size [13]. A very small particle size increases the free energy of the system and could again lead to instability. If the suspension is a parentral preparation then the syringibility also depends on the particle size [10].

Micronization and subsequent drying of a wet mass decreases the time required for the process. Drying also occurs in a very uniform manner [10]. Recent advances in the pharmaceutical industry include the administration of the drug through the nasal route. If the particle size exceeds critical dimensions the particle is retained in the upper respiratory tract and is then swallowed into the GIT, where its bioavailability greatly decreases. The position and retention of the drug particles in the bronchopulmonary systems is determined mainly by the size of the particles [15].

Grinding is of utmost importance in tablets and capsule manufacture, since their formulation consists of a mixture of powders. If the sample consists of powders of different particle size, it causes segregation of particles in the hopper during tablet manufacture. The larger particles tend to drift upwards while the smaller particles downward. This causes weight variation and poor content uniformity. The ease of mixing will be enhanced if the particles are of uniform size [16]. This provides uniformity in dosing formulations. In tablet manufacture not only is the particle size of the active drug important, but the particle size of the excepients should also be controlled to ensure uniformity in the final product. When powders are tinted the particle size of the powder and the pigment affects the final color [13]. Milling is not only responsible for the size reduction but it also ensures uniform distribution of color. Smaller sized lubricant particles can coat the surface of the tablet granules more efficiently rather than large sized particles. A fine particle size is essential if the lubricant is to function properly [10]. Milling of ointments, pastes and creams not only improves their texture and appearance but also adds to their physical stability [10]. The flow properties of concentrated suspensions are also controlled by the particle size distribution [13].

Although grinding is a very useful technique, it has a few disadvantages. The reduction in particle size leads to an increase in surface area. In a number of instances this can lead to a decrease in the chemical stability [12]. This is especially true if the material is susceptible to oxidation and hydrolysis. During milling the formation of a non-crystalline surface is often encountered. This newly formed surface is highly susceptible to oxidation [11]. Thus, if oxides are subjected to intense milling then their oxygen content increases, an example being the conversion of Fe_2O_3 to Fe_3O_4 during milling [11]. A lot of the milling energy is dissipated as heat. This can be problematic with materials that tend to liquefy and stick together or are heat labile [12]. A good example would be waxes, which are heat sensitive. Another problem arises with hydrates, which under the influence of the high milling temperatures release their water of hydration [11]. If the moisture content of the material being milled exceeds 5% then it usually leads to agglomeration and effective particle size reduction is not achieved. Milling can also be a source of contamination of the material being ground. In some instances the mill wear can be so high that it can lead to a highly contaminated product [12].

3. Material and methods

3.1. Materials

The material studied was ''James White River Dolomite'' supplied by FMC Corp/PD, Newark, DE 19711. The material was subjected to two stages of milling. An initial low intensity grinding process in a ceramic ball mill followed by high-energy milling in a vibrating mill. Silicon powder was used as a reference standard in the XRD studies. The silicon powder (325 mesh, 99%, Lot No. BU19523CS) was obtained from Aldrich Chemical. Thermogravimetric (TG) studies were done on a pure magnesite sample obtained from a natural source collected by the Geology Department of The University of Toledo from Northwest Ohio.

3.2. Equipment

The original sample was subjected to two stages of grinding. An initial low energy grinding in a ceramic ball mill equipped with a General Electric AC motor. The grinding medium used was ceramic balls. The TG data discussed for this sample in the following sections did not indicate any structural damage to dolomite. Therefore, this sample from the ceramic ball mill (200 mesh) was then subjected to high-energy grinding using a 240 V agate vibrating mill. The milling chamber and the milling medium are made of agate. Both, the original sample and the ball-milled sample were subjected to size classification using a Rotap Testing Sieve Shaker.

The SDT 2960, simultaneous TGA–DTA, TA instrument with Universal Analysis for Windows, 95/NT Ver. 2.3 C was used to examine the thermal decomposition of the original and ground dolomite. An electronic flow meter from J&W Scientific, model ADM 1000 was used to regulate the flow of purge gas through the sample.

X-ray diffraction experiments were performed on a SCINTAG XDS2000 diffractometer with Cu Kα, $\lambda = 1.5406$ Å and solid-state Ge detector cooled by liquid nitrogen. The experimental conditions were as follows: 45 kV, 40 mA, divergent beam slits 2 and 4 mm, receiving slits 1 and 0.2 mm, $2\theta = 5{-}70^\circ$, continuous scan with a scan rate of 2°/min and step size of 0.03° for intensity integration. The measurements were taken at room temperature, in air and at normal pressure. The data were processed using Scintag software DMS2000, Ver. 3.43 on Microvax 3100 with Tektronix 4207 for graphical display. The Kα_2 data was stripped from the raw intensity, background subtracted and the data smoothed using ''fast Fourier filtering''. The JCPDS database (powder diffraction file from International Center for Diffraction Data, Vol. 1–47, release 1998) incorporated in the search–match program suit was used for the identifications of the components.

Scanning electron micrographs of all the samples were obtained. The scanning electron microscope (SEM) studies were performed on the JOEL JSM-6100 microscope, wherein the surface of the sample was coated with a thin, electric gold conductive film and the excitation voltage used was 10 kV.

3.3. Procedure

The original sample was first subjected to size classification using US standard testing sieves. The following set of US standard sieves was used for size classification, namely the 20, 40, 60, 80 100, 120, 140, 170, 200, 230, 250, 300 and 325-mesh sieves. A Rotap Testing Sieve Shaker was used to hasten the size classification process. The period of operation for this equipment was one and a half hours. The fraction retained on the 200-mesh sieve was used for TG, XRD and SEM studies. The original un-sieved and un-ground dolomite sample was then subjected to a milling process using a ceramic ball mill. The sample was ground for a period of 3 h. The sample obtained from the ceramic ball mill was subjected to size classification using the same process described above. The fraction obtained on the 200-mesh sieve was used for XRD, TG and SEM studies. From the results it was found that this sample did not show any significant structural damage. The fraction obtained on the 200-mesh sieve was therefore used for a second stage of high-energy milling. This process was carried out in a high-energy agate vibrating mill. The period of operation of this equipment was 24 h.

For the sake of convenience the samples will be referred to as samples A, B and C. Sample A represents the un-ground sample of 200-mesh size. Sample B represents ball-milled sample, ground for 3 h having the same mesh size of sample A. Finally, sample C represents sample B subjected to high-energy milling in an agate vibrating ball mill for a period of 24 h.

TG analysis, XRDs and SEMs were performed on the original and milled samples. In all these TG experiments the sample was heated at the rate of 10°C/min and the flow rate for the purge gas (CO_2) used was 50 ml/min. For all the XRD experiments a 10% w/w trace of silicon was introduced in each of the samples as an internal standard and then the peak intensities of the mixtures were measured on the diffractometer.

To confirm the identity and purity of the silicon powder a XRD pattern was obtained for this sample alone and the peak positions were compared with the values from the database. An additional TG run was performed on pure magnesite in an atmosphere of CO_2. The experimental conditions for this run were the same as those for the dolomite samples described above. The rationale for this step is justified in the following section.

4. Results and discussion

4.1. Silicon powder: XRD study

XRD data were first obtained from the database. The JCPDS card #27-1402 indicates that there are 11 peaks

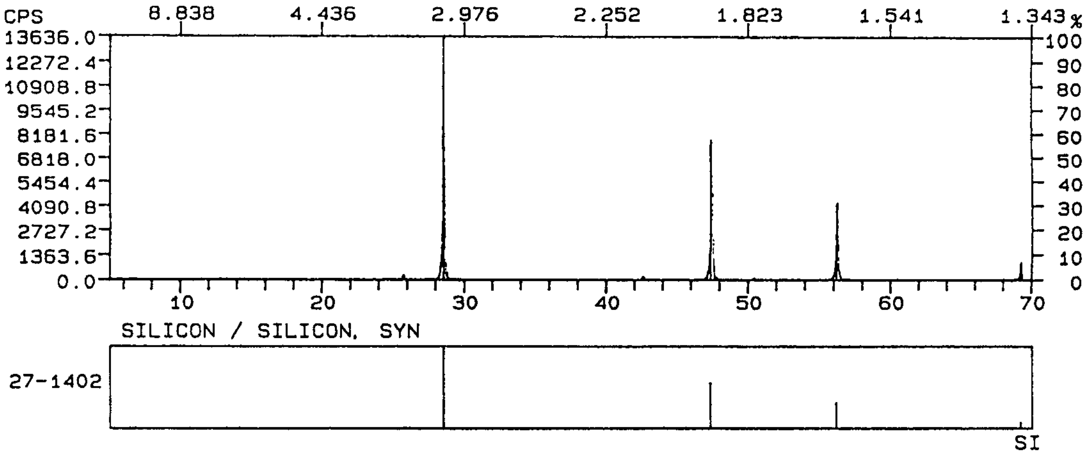

Fig. 1. X-ray diffraction pattern for silicon powder. The purity of the sample was confirmed using the JCPDS database, which indicates presence of a single component, i.e. silicon.

Table 1
Silicon peak data from the database compared to the experimentally obtained values (the sets of figures are in good agreement with one another)

Silicon peak data from the JCPDS card #27-1402		Silicon peak data from the experimental values (no correction applied)		ΔD^a
d-spacing (Å)	Relative intensity	*d*-spacing (Å)	Relative intensity	
3.135	100	3.128	100	0.007
1.920	55	1.917	66	0.003
1.637	30	1.635	35	0.002
1.375	6	1.356	8	0.019

[a] Systemic shift indicates experimental error in manual loading to be averaged ΔD ~ 0.008.

in the reflection pattern of silicon. Since the sample was scanned in the region 5–70 2θ, only 4 of these 11 peaks fall in the scanned region. The database results for this silicon sample indicate that this material is indeed pure silicon (Fig. 1). The experimental 2θ values are compared with the values from the database in Table 1 and the two sets of values are in good agreement.

4.2. TG–DTA results

The TG plot (% wt. vs. temperature) for the thermal decomposition of sample A, in an atmosphere of carbon dioxide, showed a two-stage process (Fig. 2). This is in agreement with the literature [17]. In an atmosphere of carbon dioxide the decomposition of

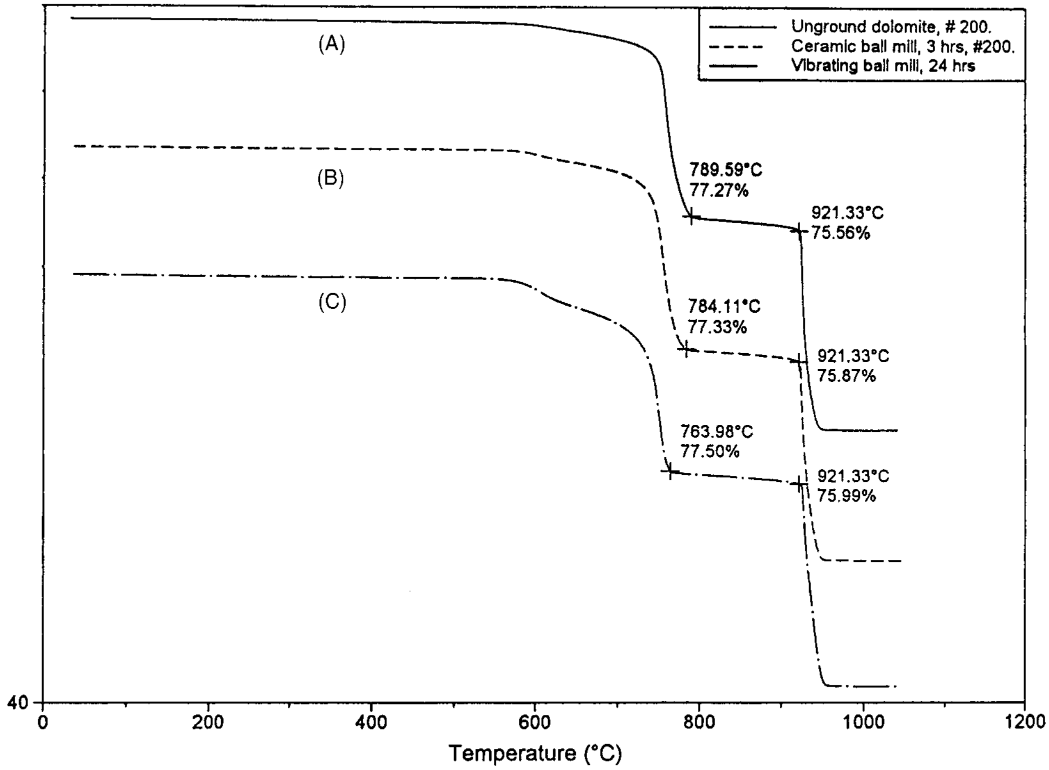

Fig. 2. TG plot for thermal decomposition of samples A, B and C at a heating rate of 10°C/min. The purge gas used in all these runs was carbon dioxide and the flow rate used was 50 ml/min. The plot indicates that as the grinding time increases the width of the plateau also increases. To estimate the percent loss for the *Y*-axis 1 cm = 6.626% weight loss.

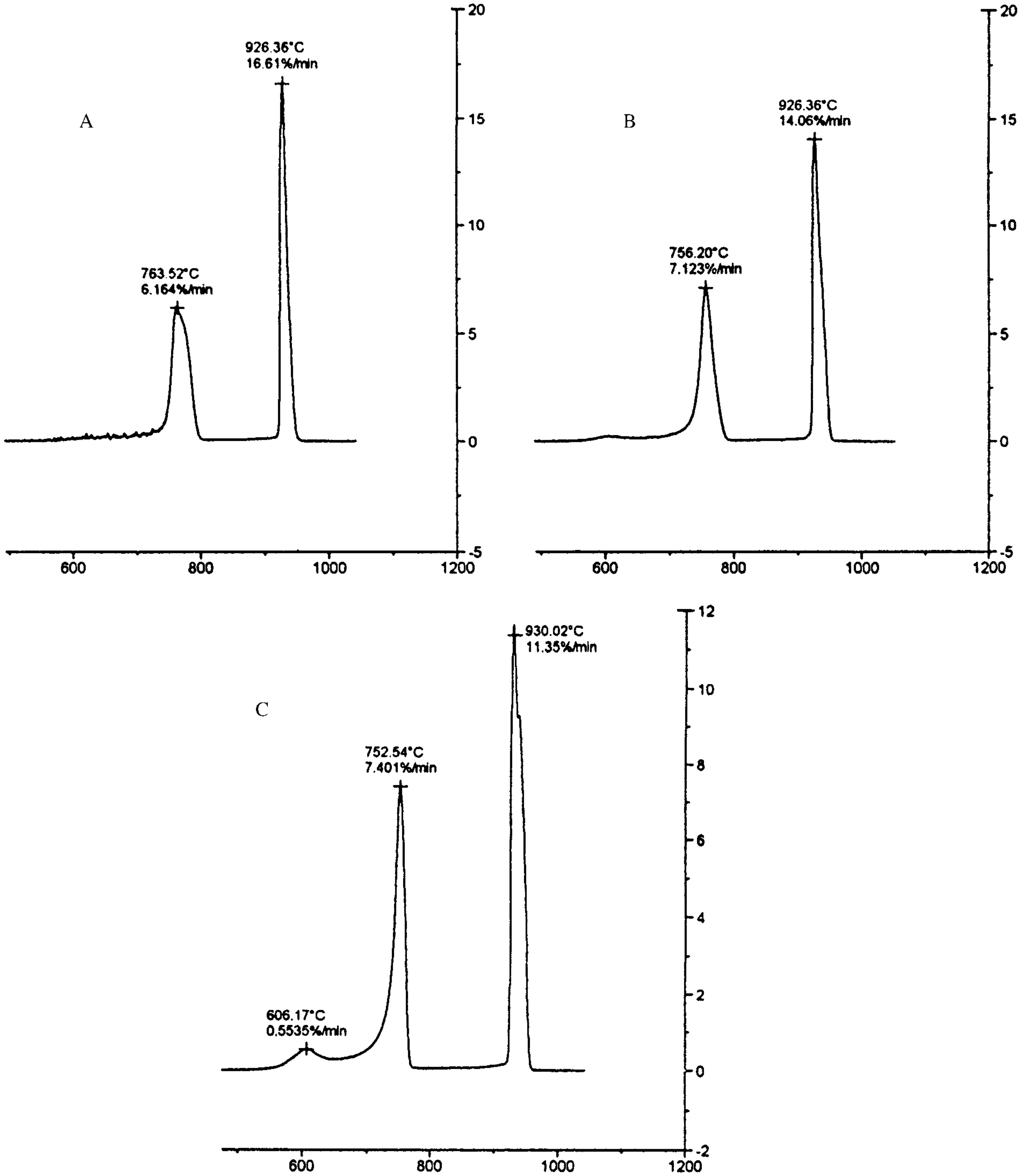

Fig. 3. DTG (% wt./min. vs. temperature) plots for the thermal decomposition of samples A, B, and C at a heating rate of 10°C/min. The purge gas used in all these runs was carbon dioxide and the flow rate used was 50 ml/min. Sample C shows an additional endotherm indicating structural damage due to intensive grinding.

dolomite occurs via a two-stage mechanism, which is depicted as follows:

$$\mathrm{CaMg(CO_3)_2 \rightarrow CaO_3 + MgO + CO_2} \quad (5)$$

$$\mathrm{CaCO_3 \rightarrow CaO + CO_2} \quad (6)$$

The DTG plot (derv. wt. vs. temperature) shows two endotherms corresponding to each of the above two reactions (Fig. 3).

The TG/DTG (Figs. 2 and 3) plots for sample B do not show any distinct change when compared to the plots of sample A. The normal two-stage decomposition of dolomite is clearly evident. This indicates that the grinding period of 3 h in a low energy mill such as a ceramic ball mill is not sufficient to bring about a change in the crystal structure of dolomite.

Sample C shows a distinct change in the DTG plot (Fig. 3). A third peak appears just before the magnesium carbonate portion of dolomite structure breaks down. This has a peak temperature of 606°C. This peak is a genuine peak and also occurs as an endotherm in the DTA (differential thermal analysis) pattern (Fig. 4). This temperature is in the decomposition region for pure magnesite. Looking at the position of this peak, it was first thought that this peak occurred because grinding led to the breakdown of the structure into individual carbonates. To test this hypothesis a run on pure magnesite was performed in an atmosphere of CO_2. The DTG plot shows that pure magnesite has a peak decomposition temperature of 644°C (Fig. 5). The difference in the above temperatures indicates that this peak is due to a structural strain in the dolomitic structure and not because of separated magnesite. Thus, to define this structural alteration in more depth and to investigate the cause of this new third peak, a detailed XRD study was carried out on all the three samples using silicon powder as an internal standard (Table 2).

4.3. X-ray powder diffraction study

The XRD study is summarized in Fig. 6. After applying the internal standard correction, it was found

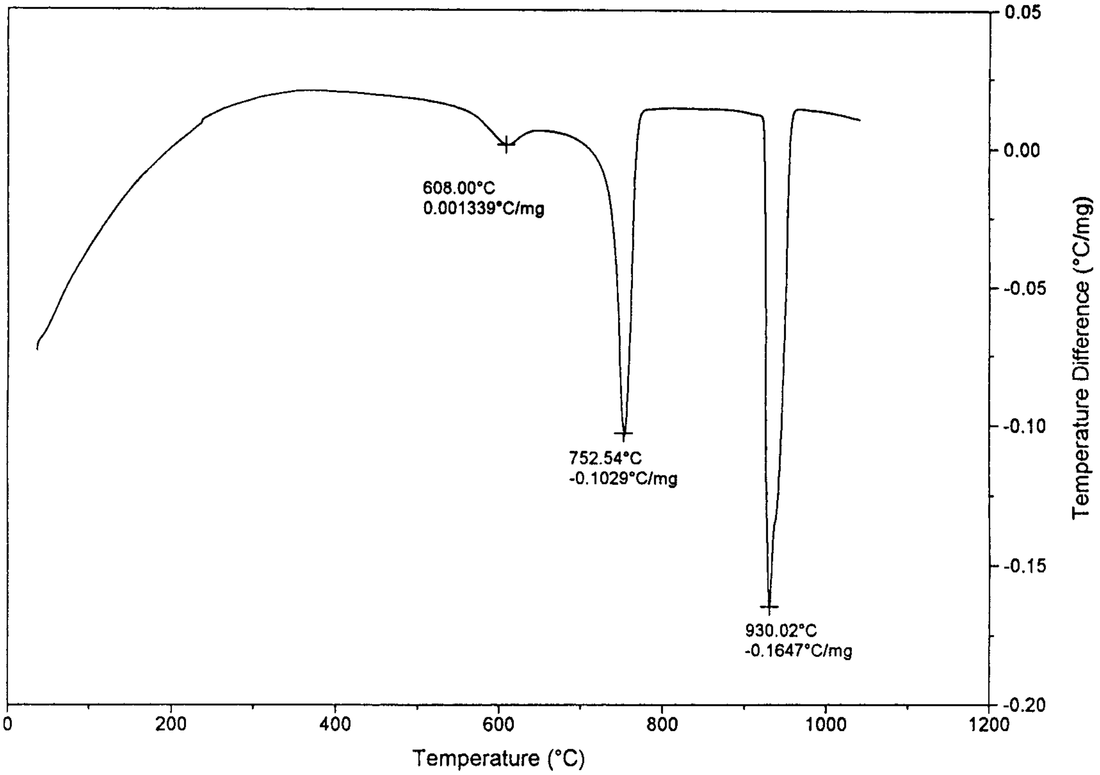

Fig. 4. DTA pattern for sample C, confirming the genuineness of the peak observed in the DTG plot of the same sample.

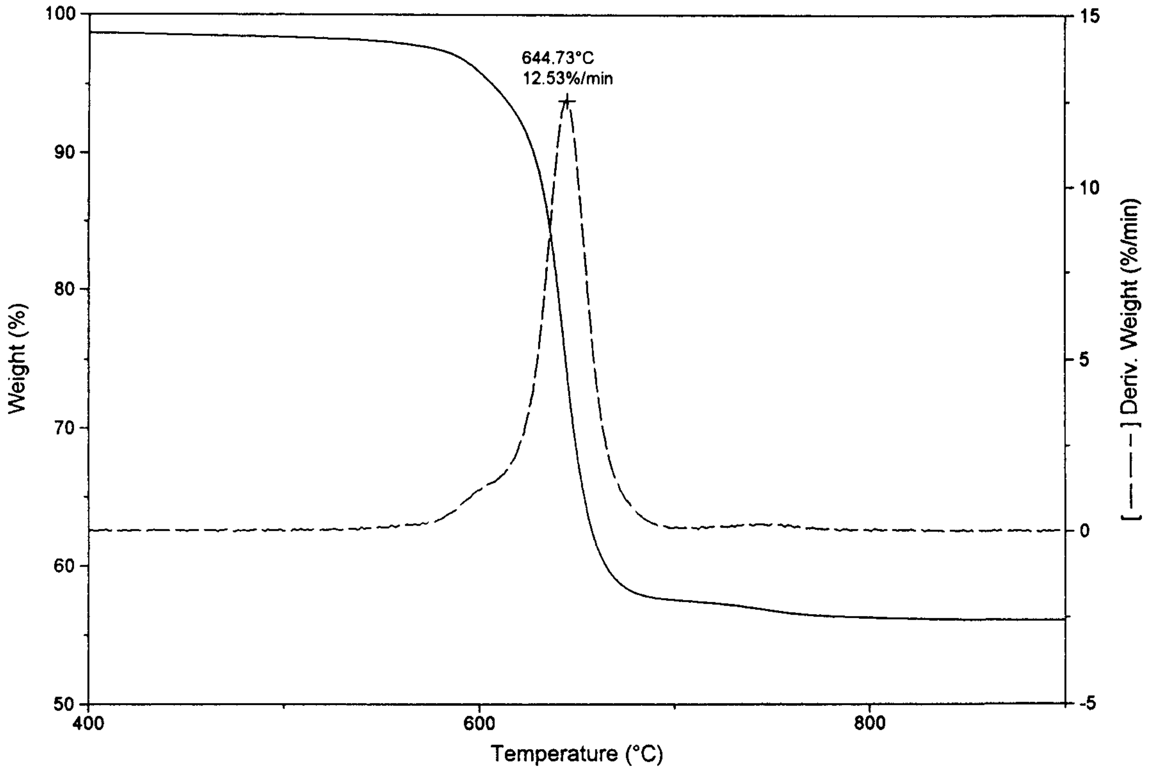

Fig. 5. TG/DTG plots for the thermal decomposition of magnesite in an atmosphere of CO_2. Heating rate employed was 10°C/min and the flow rate of the purge gas was 50 ml/min.

that the peaks of dolomite in the XRD pattern have not altered. There is neither any alteration in the peak intensity nor in the peak position. This indicates that the unit cell of dolomite is still intact after the intensive grinding operation in the vibrating agate mill. There is probably a strain introduced in the dolomitic structure and this strain is associated with the magnesium carbonate part of dolomite. This strain in the structure is not detectable by the XRD methodology used in this study.

If the dolomite sample could be subjected to an even greater mechanical grinding process then the strain would become more obvious and might be detectable by the X-ray analysis.

4.4. SEM study

Sample A (Fig. 7) shows the presence of discrete grains with some grains having sharp edges. This sample is an un-ground sample and therefore exhibits normal thermal decomposition behavior. In the case of sample B, the first step in the thermal decomposition shows an initial slow reaction, which then proceeds at a faster rate at higher temperatures. The SEM reported on this sample (Fig. 8) indicated the reason for this. The SEM indicated the presence of fine fluffy dolomite particles sticking to the dolomite crystals. This fluffy matter decomposes earlier as compared to the crystals and this causes an initial slow reaction followed by the increase in the reaction rate when the intact grains begin to decompose. Sample C (Fig. 9) shows the presence of large aggregates. This is an expected phenomenon. Whenever a material is ground excessively the surface area increases tremendously. This leads to an increase in the surface energy. Particles in an attempt to reduce this excess free surface energy begin to agglomerate and hence the SEM shows the

Table 2
Comparison of the *d*-spacing values for the three samples after applying a correction by using silicon as an internal standard (the italic figures are the silicon peaks in each of the samples)

hkl for dolomite from JCPDS database, card #36-426	*d*-spacing (Å) from the JCPDS database, card #36-426, 27-1402	*d*-spacing (Å) un-ground dolomite, sample A (#200)	*d*-spacing (Å) ground samples, the number of hours indicate grinding time	
			Sample B: ceramic ball mill (#200) 3 h	Sample C: vibrating mill 24 h
012	3.699	3.694	3.694	3.694
	3.135	*3.135*	*3.135*	*3.135*
104	2.888	2.886	2.886	2.885
006	2.670	2.668	2.669	2.668
015	2.539	2.538	2.538	2.538
110	2.404	2.404	2.404	2.404
113	2.193	2.192	2.192	2.192
021	2.065	2.064	2.064	2.065
202	2.015	2.015	2.015	2.014
	1.920	*1.920*	*1.920*	*1.920*
024	1.847	1.847	1.847	1.847
018	1.805	1.804	1.804	1.803
116	1.787	1.786	1.786	1.786
	1.637	*1.637*	*1.637*	*1.637*
211	1.566	1.566	1.566	1.566
122	1.544	1.544	1.544	1.544
214	1.465	1.464	1.464	1.464
208	1.443	1.443	1.443	1.442
119	1.431	1.430	1.430	1.429
300	1.388	1.387	1.387	1.387
	1.357	*1.357*	*1.357*	*1.357*

presence of large aggregates having no definite shape.

4.5. Effect of grinding time on the plateau portion of the TG curve

The partial pressure of CO_2 causes the two stages in the thermal decomposition of dolomite to separate out distinctly [17]. Because the two stages are distinctly separated the TG plot shows an intermediate plateau region where practically no weight loss occurs. Upon observing Fig. 2 more closely it is found that the width of this plateau increases with grinding time. The temperature difference between the completion of stage 1 and the onset of stage 2 for samples A, B and C were found to be 131, 137 and 158°C, respectively.

The second stage onset temperature remains unaffected in all the three samples while the first stage occurs at progressively lower temperatures with an increase in grinding time. This can be explained based on the fact that grinding causes surface activation. The ground material is in an activated state having elevated energy levels and therefore the reaction occurs with lower input of energy. This implies that the reaction temperature will go down and the plateau width will increase as a secondary effect of this process.

The reason why the second stage is independent of grinding time is because it is a reversible reaction. In other studies performed by us, involving various flow rates of the purge gas and different heating rates, it was always found that this second stage occurs at a fixed temperature of around 920°C. The reaction remains reversible up to a certain point and beyond this point the reaction can no longer sustain the energy intake. Therefore, the second stage of decomposition occurs at a drastic rate. The point of degradation remains constant and is not affected by any variation in program design or procedural variables.

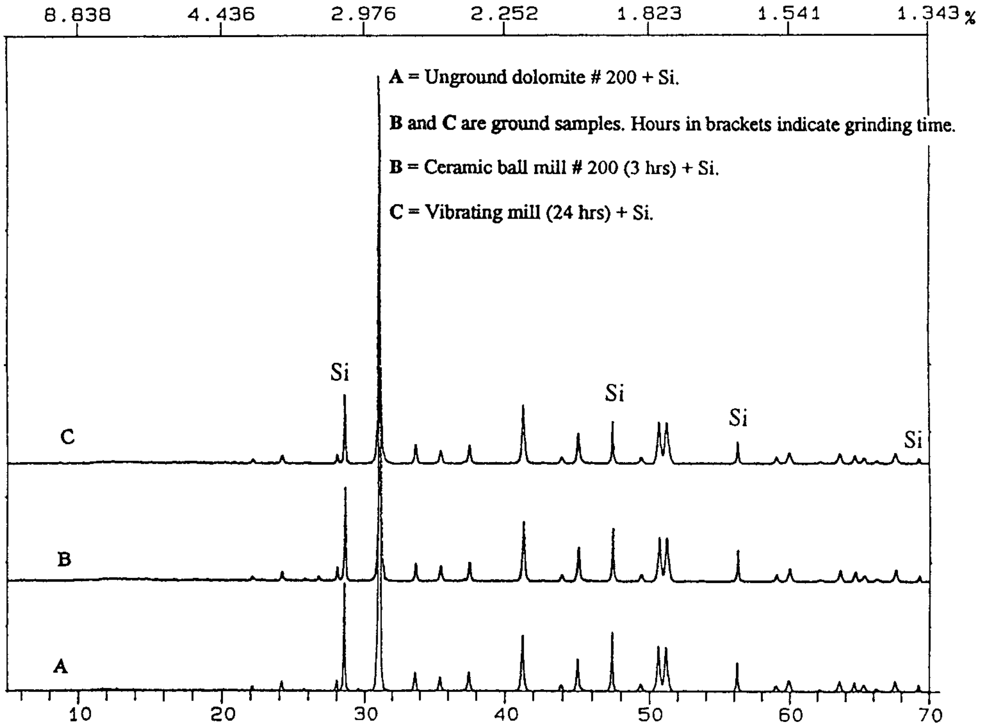

Fig. 6. The XRD pattern for samples A, B, and C after application of a correction by using silicon as an internal standard. It is difficult to distinguish any changes in the structure using the XRD, as peaks after application of the correction have neither shifted, nor have the intensities of the peaks altered. The *d*-spacing is plotted on the upper scale, while the 2θ is plotted on the bottom scale.

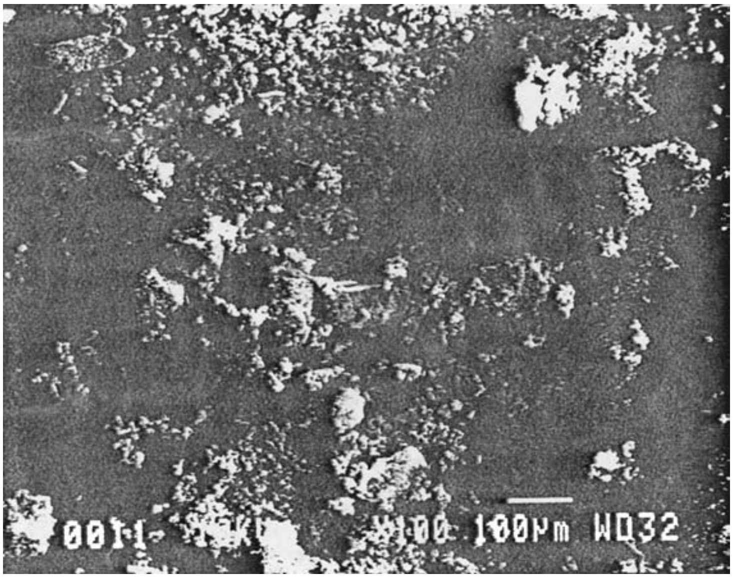

Fig. 7. SEM of sample A using a magnification of 100× and excitation voltage of 10 kV.

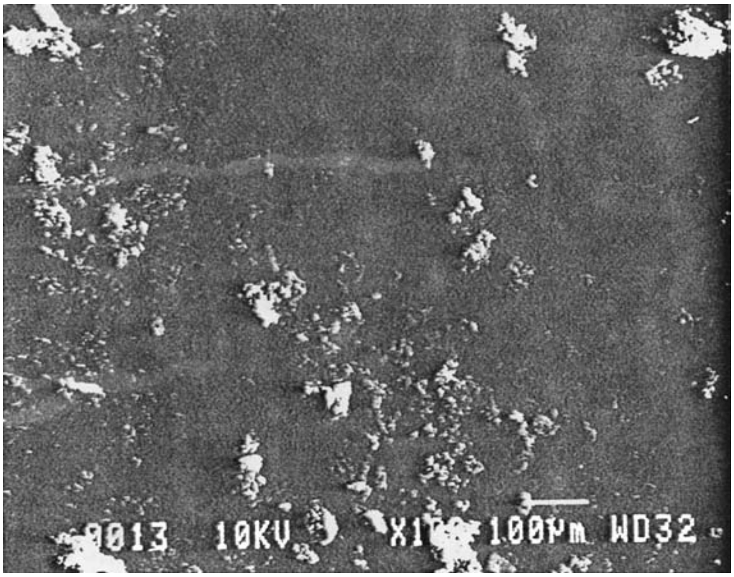

Fig. 8. SEM of sample B using a magnification of 100× and excitation voltage of 10 kV.

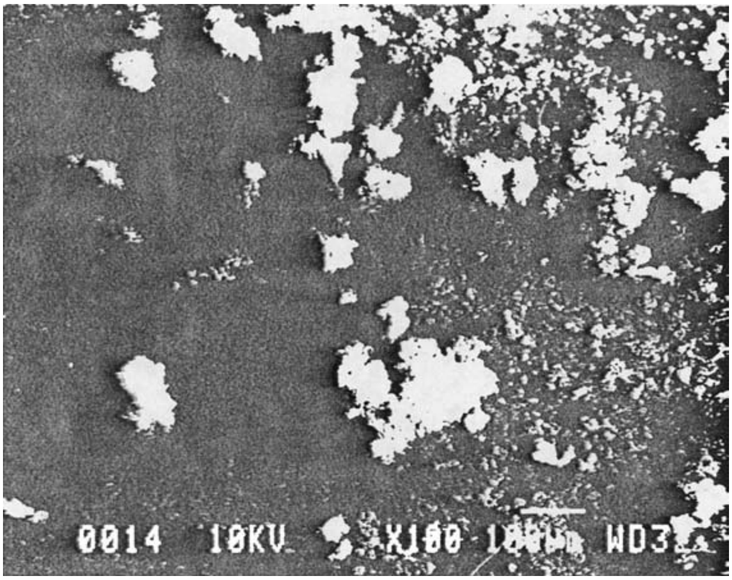

Fig. 9. SEM of sample C using a magnification of 100× and excitation voltage of 10 kV.

5. Conclusions

1. Grinding results in surface activation of the material, which leads to a lowering of the decomposition temperature. This was observed for the first stage thermal decomposition of dolomite. The second stage remains unaffected.
2. Surface activation leads to an increase in the surface free energy of the system. The ground particles then begin to agglomerate in an attempt

to decrease this free energy. This was observed in the SEM of sample C.

3. The unit cell of dolomite remains intact even after 24 h of grinding. However, the grinding causes irreversible crystal structure alteration in dolomite, which in turn affects its thermal properties. This change in thermal property (a third peak in both DTG and DTA) is due to structural strain and not due to surface activation or particle size reduction. This strain remains undetected in the XRD pattern. If a more powerful grinding equipment were available then the measure of the induced strain would be considerably higher and this structural change might then become evident in the XRD pattern. The XRD methodology described here can be used for an in-depth study of intensively ground dolomites and can yield useful information. For future work, high-energy equipment coupled with the XRD analysis described here could conclusively describe the nature and structural pattern of ground dolomites.

References

[1] K.V. Nair, Masters Thesis, The University of Toledo, August 1994, p. 1.

[2] B. Bilinski, E. Stefaniak, P. Stasczuk, Powder Technol. 73 (1992) 261–266.

[3] É. Kristóf, A.Z. Jahász, Powder Technol. 75 (1993) 145–152.

[4] R. Ozao, M. Ochiai, A. Yamazaki, R. Otsuka, Thermochim. Acta 183 (1991) 183–198.

[5] Y. Arai, T. Yasue, Kogyo Kagaku Zasshi 72 (1969) 1980.

[6] Y. Arai, T. Yasue, Gypsum Lime 103 (1969) 319.

[7] Y. Arai, T. Yasue, Gypsum Lime 104 (1970) 17.

[8] W.F. Bradley, J.F. Burst, D.L. Graf, Am. Mineral. 38 (1953) 207.

[9] V.I. Molchanov, Mekhan. Yavl. Svekhtonkom. Izmel. Chem. (1971) 155.

[10] L. Lachman, H.A. Lieberman, J.L. Kanig, Lea & Febiger, 3rd Edition, Philadelphia, PA, 1986, pp. 21, 22, 31, 32, 180.

[11] J. Šestak, Thermophysical properties of solids, in: G. Svehla (Ed.), Comprehensive Analytical Chemistry, Vol. XII, Part D, Elsevier, Amsterdam, 1984, pp. 20, 21.

[12] A. Felmeister, Remington's Pharmaceutical Sciences, 15th Edition, Mack Publishing Co., Easton, PA, 1975, pp. 1554–1557.

[13] D. Ganderton, A.J. Hickey, Unit processes in pharmacy: the operations to zeta potential, in: J. Swarbrick, J.C. Boylan (Eds.), Encyclopedia of Pharmaceutical Technology, Vol. 16, Marcel Dekker, New York, pp. 66, 67.

[14] M. Kraml, J. Dubue, R. Gaudry, Antibiot. Chemother. 12 (1962) 232.

[15] J. Kanig, J. Pharmceut. Sci. 52 (1963) 513.

[16] E.L. Parrot, Drug Cosm. Inc. 115 (1974) 42.

[17] W.R. Bandi, G. Krapf, Thermochim. Acta 14 (1976) 221.